Electronic Supplementary Material (ESI) for CrystEngComm.

Metal-organic and Supramolecular Lead(II) Networks Assembled from Isomeric Nicotinoylhydrazone Blocks: The Effects of Ligand Geometry and Counter-ion on Topology and Supramolecular Assembly

Ghodrat Mahmoudi, Antonio Bauzá, Antonio Frontera, Piotr Garczarek, Najah Mhesn, Christos Lampropoulos, Vladimir Stilinović

SUPPLEMENTARY INFORMATION

Table S1 Crystallographic data for **1-6**

Compound	**1**	**2**	**3**
Formula	$C_{13}H_{12}Cl_2N_4OPb$	$C_{13}H_{12}Cl_2N_6O_7Pb$	$C_{30}H_{24}N_{12}O_2Pb_2S_4$
Formula weight	518.36	571.48	1127.23
Temperature / K	100(2)	100(2)	123(2)
Wavelength / nm	0.71073 Å	0.71073 Å	0.71073 Å
Crystal system	Monoclinic	Triclinic	Triclinic
Space group	$P2_1/c$	$P\bar{1}$	$P\bar{1}$
Unit cell dimensions			
a / Å	10.4863(14)	9.0862(4)	7.5527(2)
b / Å	14.790(2)	9.3122(4)	14.5337(5)
c / Å	10.8544(15)	11.5175(5)	16.8369(4)
α / °	90	84.9050(10)	102.817(2)
β / °	116.161(2)	72.8090(10)	94.897(2)
γ / °	90	62.7750(10)	98.141(2)
Volume / Å^3	1511.0(4)	826.61(6)	1770.85(9)
Z	4	2	2
$D_{calculated}$ / g cm^{-3}	2.279	2.296	2.114
μ / mm^{-1}	11.522	10.259	9.779
F(000)	968	540	1064
Crystal size / mm^3	0.22 × 0.19 × 0.15	0.23 × 0.17 × 0.10	0.60 × 0.15 × 0.11
Theta range for data collection/°	2.16 – 29.18	2.46 – 29.14	3.13–30.24°
Index ranges	$-14 \le h \le 14$	$-11 \le h \le 12$	$-9 \le h \le 9$
	$-19 \le k \le 20$	$-12 \le k \le 12$	$-19 \le k \le 19$
	$-14 \le l \le 14$	$-15 \le l \le 15$	$-22 \le l \le 22$
Reflections collected	26047	14331	25546
Independent reflections	3940	3973	8516
Refinement method	Full matrix	Full–matrix	Full–matrix
	least squares on F^2	least–squares on F^2	least–squares on F^2
Data / restraints / parameters	3940/0/191	3973/0/245	8516/0/461
Goodness–of–fit on F^2	1.032	1.079	1.059
Final R indices [$I>2\sigma(I)$] R_1 =	0.0183	0.0192	0.0248
wR_1 =	0.0403	0.0484	0.0425
R Indices (all data) R_2 =	0.0223	0.0198	0.0248
wR_2 =	0.0418	0.0487	0.0454
$\Delta\rho$ / e Å^{-3}	1.420, –0.802	2.220, –1.173	0.691 – 0.716

Table S1 continued

Compound	**4**	**5**	**6**
Formula	$C_{13}H_{12}Cl_2N_4OPb$	$C_{13}H_{12}Cl_2N_6O_7Pb$	$C_{15}H_{12}N_6OPbS_2$
Formula weight	518.36	571.48	563.62
Temperature / K	150(2)	100(2)	293(2)
Wavelength / nm	0.71073 Å	0.71075	0.71073 Å
Crystal system	Triclinic	Monoclinic	Triclinic
Space group	$P\bar{1}$	$P2_1/c$	$P\bar{1}$
Unit cell dimensions			
a / Å	7.8658(7)	9.0537(3)	8.6135(4)
b / Å	8.6864(7)	23.1055(8)	9.3532(7)
c / Å	11.0020(9)	7.8698(3)	11.1952(10)
α / °	100.321(4)	90.00	87.356(7)
β / °	92.891(4)	98.4580(10)	87.566(5)
γ / °	95.189(4)	90.00	82.906(5)
Volume / Å^3	734.82(11)	1628.38(10)	893.46(11)
Z	2	4	2
$D_{calculated}$ / g cm^{-3}	2.343	2.331	2.095
μ / mm^{-1}	11.846	10.416	9.691
F(000)	484	1080	532
Crystal size / mm^3	0.71× 0.18 × 0.10	0.16 × 0.05× 0.05	0.08 × 0.04 × 0.02
Theta range for data collection/°	2.40 – 28.28	1.76 – 33.17	2.91 – 28.60
Index ranges	$-10 \le h \le 10$	$-13 \le h \le 13$	$-11 \le h \le 11$
	$-11 \le k \le 11$	$-35 \le k \le 32$	$-10 \le k \le 12$
	$-14 \le l \le 14$	$-12 \le l \le 11$	$-15 \le l \le 14$
Reflections collected	18736	29363	8887
Independent reflections	3653	6193	4459
Refinement method	Full–matrix	Full matrix	Full matrix
	least–squares on F^2	least squares on F^2	least squares on F^2
Data / restraints / parameters	3653/0/190	6193/0/245	4459/0/227
Goodness–of–fit on F^2	1.053	0.996	1.147
Final R indices [$I>2\sigma(I)$] R_1 =	0.0177	0.0291	0.0319
wR_1 =	0.0455	0.0586	0.0773
R Indices (all data) R_2 =	0.0187	0.0437	0.0363
wR_2 =	0.0461	0.0624	0.0793
$\Delta\rho$ / e Å^{-3}	1.046, –1.750	1.614, –2.063	1.901, –1.146

Table S2. Selected bond lengths and angles in the structure of **1**.

Bond lenghts / Å			
Pb1-Cl1	2.9279(8)	Pb1-Cl2	2.7027(8)
Pb1-Cl2^{i}	3.1048(8)	Pb1-O1	2.5858(19)
Pb1-N1	2.640(2)	Pb1-N2	2.739(2)
Pb1-N4^{ii}	2.841(2)		
Bond angles / º			
O1-Pb1-N1	118.87(6)	O1-Pb1Cl2	84.84(5)
N1-Pb1-Cl2	86.37(5)	O1-Pb1-N2	59.53(6)
N1-Pb1-N2	59.50(7)	Cl2-Pb1-N2	77.43(5)
O1-Pb1-N4^{ii}	70.67(6)	N1-Pb1-N4^{ii}	168.08(6)
Cl2-Pb1-N4^{ii}	87.53(5)	N2-Pb1-N4^{ii}	128.79(6)
O1-Pb1-Cl1	152.84(4)	N1-Pb1-Cl1	86.47(5)
Cl2-Pb1-Cl1	87.45(2)	N2-Pb1-Cl1	143.16(5)
N4^{ii}-Pb1-Cl1	83.03(5)	O1-Pb1-Cl2^{i}	83.74(5)
N1-Pb1-Cl2^{i}	83.20(5)	Cl2-Pb1-Cl2^{i}	158.40(2)
N2-Pb1-Cl2^{i}	80.98(5)	N4ii-Pb1-Cl2^{i}	105.78(5)

Symmetry codes – i: x, 1.5-y, 0.5+z; ii: 1-x, 2-y, 1-z;

Table S3. Selected bond lengths (Å) and angles (º) in the structure of **2**.

Bond lengths			
Pb1-O1	2.511(2)	Pb1-O2	2.520(2)
Pb1-O3	2.757(2)	Pb1-O5	2.708(2)
Pb1-O7^{i}	2.867(2)	Pb-N1	2.531(2)
Pb1-N2	2.638(2)		
Bond angles			
O1-Pb1-O2	77.47(7)	O1-Pb1-N1	122.24(7)
O2-Pb1-N1	77.66(8)	O1-Pb1-N2	61.10(7)
O2-Pb1-N2	69.60(7)	N1-Pb1-N2	61.50(8)
O1-Pb1-O5	73.45(7)	O2-Pb1-O5	132.44(6)
N1-Pb1-O5	87.03(7)	N2-Pb1-O5	63.57(7)
O1-Pb1-O3	117.79(8)	O2-Pb1-O3	48.46(7)
N1-Pb1-O3	78.86(8)	N2-Pb1-O3	112.06(7)
O5-Pb1-O3	165.28(8)	O1-Pb1-O7^{i}	149.81(7)
O2-Pb1-O7^{i}	119.13(7)	N1-Pb1-O7^{i}	87.22(7)
N2-Pb1-O7^{i}	145.97(7)	O5-Pb1-O7	104.50(6)
O3-Pb1-O7^{i}	70.90(7)		

Symmetry code - i: 2-x, 1-y, -z;

Table S4. Selected bond lengths (Å) and angles (º) in the structure of **3**.

Bond lenghts			
Pb1-N10	2.506(3)	Pb1-O1	2.525(3)
Pb1-N3	2.550(3)	Pb1-N1	2.575(3)
Pb1-S1	3.002(1)	Pb2-O2	2.518(3)
Pb2-N7	2.635(3)	Pb2-N12	2.667(3)
Pb2-N5	2.710(3)	Pb2-N4	2.763(3)
Pb2-S3	2.8335(9)		
Bond angles			
N10-Pb1-O1	78.73(10)	N10-Pb1-N3	79.33(9)
O1-Pb1-N3	124.29(9)	N10-Pb1-N1	73.34(10)
O1-Pb1-N1	62.42(8)	N3-Pb1-N1	62.36(10)
N10-Pb1-S1	152.23(8)	O1-Pb1-S1	88.73(6)
N3-Pb1-S1	87.78(6)	N1-Pb1-S1	78.90(7)
O2-Pb-N7	119.61(9)	O2-Pb2-N12	149.38(9)
N7-Pb2-N12	83.35(10)	O2-Pb2-N5	60.22(8)
N7-Pb2-N5	59.72(9)	N12-Pb2-N5	134.33(10)
O2-Pb2-N4	74.55(8)	N7-Pb2-N4	160.33(9)
N12-Pb2-N4	78.91(10)	N5-Pb2-N4	130.31(9)
O2-Pb2-S3	88.86(6)	N7-Pb2-S3	84.88(7)
N12-Pb2-S3	72.29(8)	N5-Pb2-S3	78.14(6)
N4-Pb2-S3	81.70(6)		

Table S5. Selected bond lengths (Å) and angles (º) in the structure of **4**.

Bond lenghts			
Pb1-Cl1	2.7461(7)	Pb1-Cl1^{i}	2.9223(8)
Pb1-Cl2	2.7961(8)	Pb1-O1^{ii}	2.794(2)
Pb1-N1	2.713(3)	Pb1-N4^{iii}	2.588(2)
Bond angles			
N4^{iii}-Pb1-N1	162.09(8)	N4^{iii}-Pb1-Cl1	81.82(6)
N1-Pb1-Cl1	80.91(6)	N4^{iii}-Pb1-O1^{ii}	75.30(7)
N1-Pb1-O1^{ii}	119.47(7)	Cl1-Pb1-O1	151.47(5)
N4^{iii}-Pb1-Cl2	88.23(6)	N1-Pb1-Cl2	97.47(6)
Cl1-Pb1-Cl2	93.36(2)	O1^{ii}-Pb1-Cl2	102.61(5)
N4^{iii}-Pb1-Cl1^{i}	85.65(6)	N1-Pb1-Cl1^{i}	87.41(6)
Cl1-Pb1-Cl1^{i}	82.40(2)	O1^{ii}-Pb1-Cl1^{i}	79.13(5)
Cl2-Pb1-Cl1^{i}	173.00(2)	Pb1-Cl1-Pb1^{i}	97.60(2)

Symmetry codes – i: 1-x, 1-y, -z; ii: 1-x, 1-y, 1-z; iii: x, 1+y, -1+z;

Table X5. Selected bond lengths (Å) and angles (º) in the structure of **5**.

Bond lenghts			
Pb1-O1^{i}	2.551(2)	Pb1-O2	2.700(2)
Pb1-O3	2.641(3)	Pb1-O5	2.792(2)
Pb1-O6^{i}	2.874(2)	Pb1-O7^{i}	2.705(2)
Pb1-N1	2.776(3)	Pb1-N4^{ii}	2.722(3)
Bond angles			
O1^{i}-Pb1-O3	70.64(8)	O1^{i}-Pb1-O2	102.37(8)

O3-Pb1-O2	47.71(7)	O1^{i}-Pb1-O7^{i}	69.65(7)
O3-Pb1-O7^{i}	135.92(7)	O2-Pb1-O7^{i}	162.15(7)
O1^{i}-Pb1-N4^{ii}	72.57(7)	O3-Pb1-N4^{ii}	90.85(8)
O2-Pb1-N4^{ii}	67.30(8)	O7^{i}-Pb-N4^{ii}	94.88(7)
O1^{i}-Pb1-N1	140.30(7)	O3-Pb1-N1	78.01(8)
O2-Pb1-N1	71.58(8)	O7^{i}-Pb1-N1	124.97(8)
N4^{ii}-Pb1-N1	132.61(8)	O1^{i}-Pb1-O5	117.67(7)
O3-Pb1-O5	154.37(7)	O2-Pb1-O5	107.31(7)
O7^{i}-Pb1-O5	65.48(7)	N4^{ii}-Pb1-O5	70.67(8)
N1-Pb1-O5	101.14(8)	O1^{i}-Pb1-O6^{i}	108.40(7)
O3-Pb1-O6^{i}	137.99(7)	O2-Pb1-O6^{i}	148.15(7)
O7^{i}-Pb1-O6^{i}	45.85(7)	N4^{ii}-Pb1-O6^{i}	129.95(7)
N1-Pb1-O6i	79.46(7)	O5-Pb1-O6^{i}	65.18(7)

Symmetry codes – i: x, 0.5-y, -0.5+z; ii: -x, -0.5+y, 1.5-z;

Table S6. Selected bond lengths (Å) and angles (º) in the structure of **6**.

Bond lenghts			
Pb1-N5^{i}	2.525(7)	Pb1-O1	2.549(4)
Pb1-N1^{ii}	2.666(4)	Pb1-N4^{iii}	2.718(4)
Pb1-S1	3.0464(17)		
Bond angles			
N5^{i}-Pb1-O1	73.6(2)	N5^{i}-Pb-N1^{ii}	80.63(19)
O1-Pb1-N1^{ii}	75.49(13)	N5^{i}-Pb1-N4^{iii}	76.89(16)
O1-Pb1-N4^{iii}	116.78(14)	N1^{ii}-Pb1-N4^{iii}	149.38(15)
N5^{i}-Pb1-S1	94.9(3)	O1-Pb1-S1	155.66(10)
N1^{ii}-Pb1-S1	81.57(10)	N4^{iii}-Pb1-S1	79.95(10)

Symmetry codes – i: 2-x, -y, 2-z; ii: 2-x, -y, 1-z; 2-x, 1-y, 2-z;

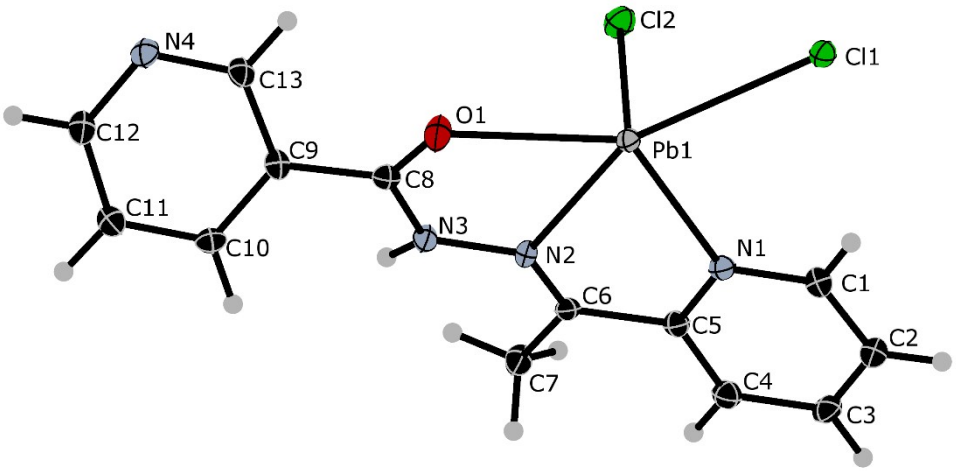

Fig. S1. Asymmetric unit of **1**. Thermal ellipsoids drawn with 50% probability

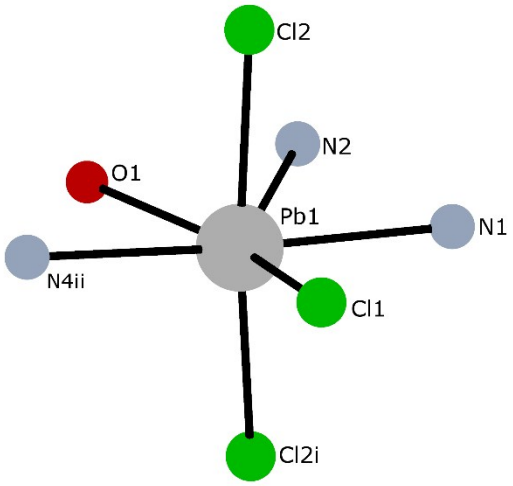

Fig. S2. Coordination environment of Pb cation in the structure of **1**.
Symmetry codes i: x, 0.5-y, 0.5+z; ii: -x, -y, -z;

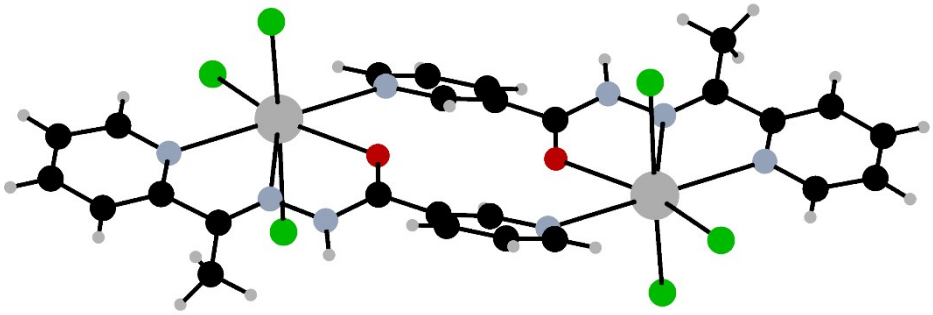

Fig. S3. Coordination subunit in the structure of **1**.

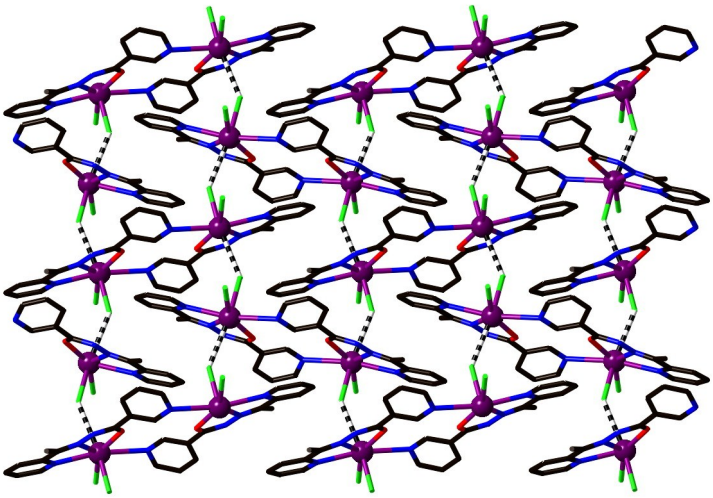

Fig. S4. The sheet structure of **1**; the longer Pb-Cl (3.105 Å) interactions are highlighted by the striped bonds.

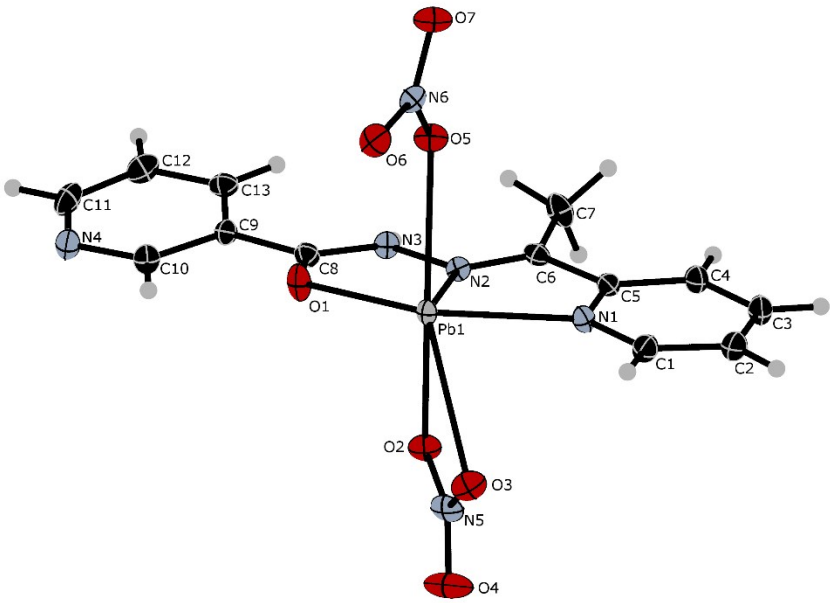

Fig. S5. Asymmetric unit of **2**. Thermal ellipsoids drawn with 50% probability.

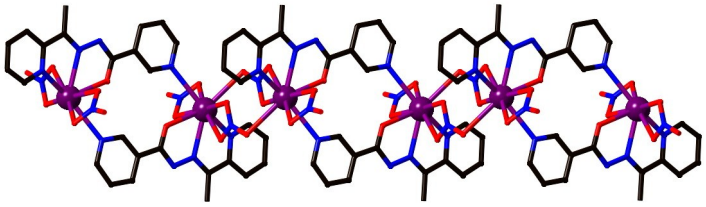

(a)

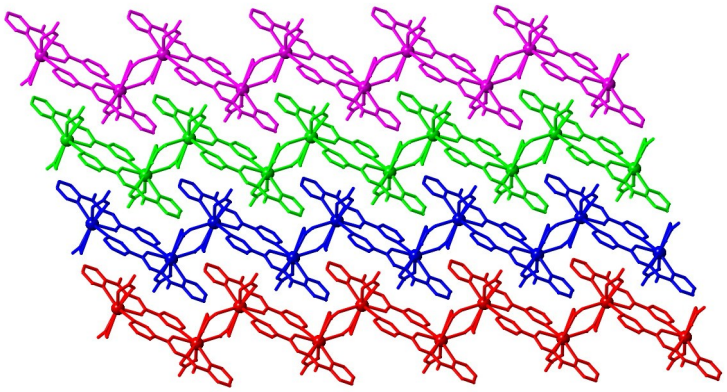

(b)

Fig. S6 (a) The structure of the 1D coordination polymer **2**. (b) A layer of chains.

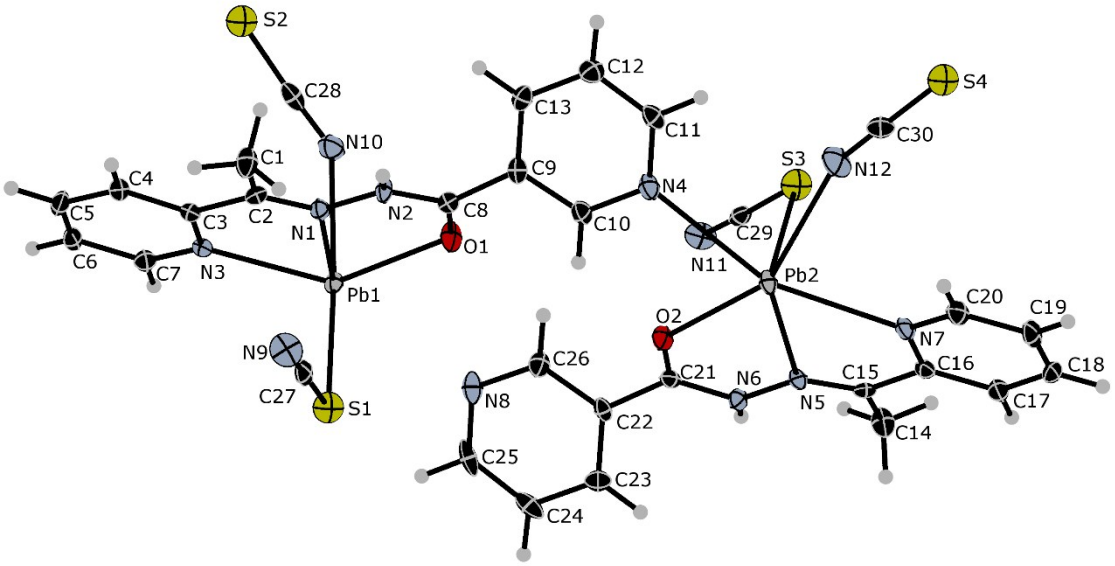

Fig. S7. Asymmetric unit of **3**. Thermal ellipsoids drawn with 50% probability.

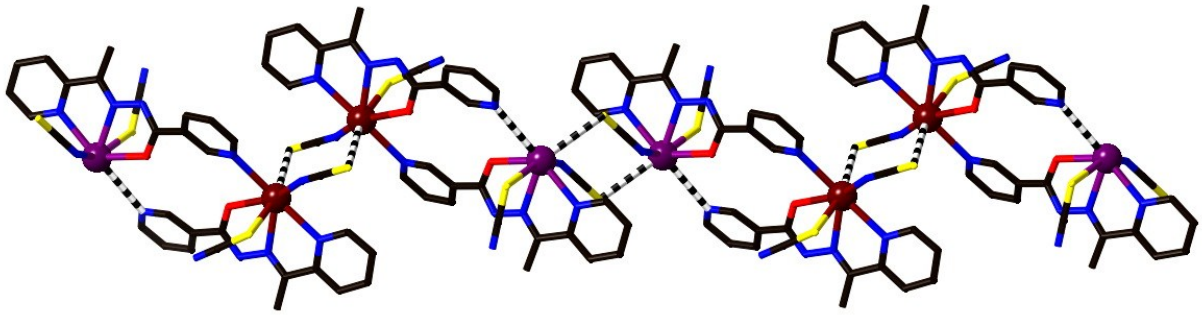

Fig S8 The assembly of dimers into 1D chains in the structure of **3**. Weaker (Pb-N/S > 3.1 Å) interactions are shown by the striped bonds. Purple spheres represent the Pb1 atoms, while the brown spheres represent the Pb2 atoms.

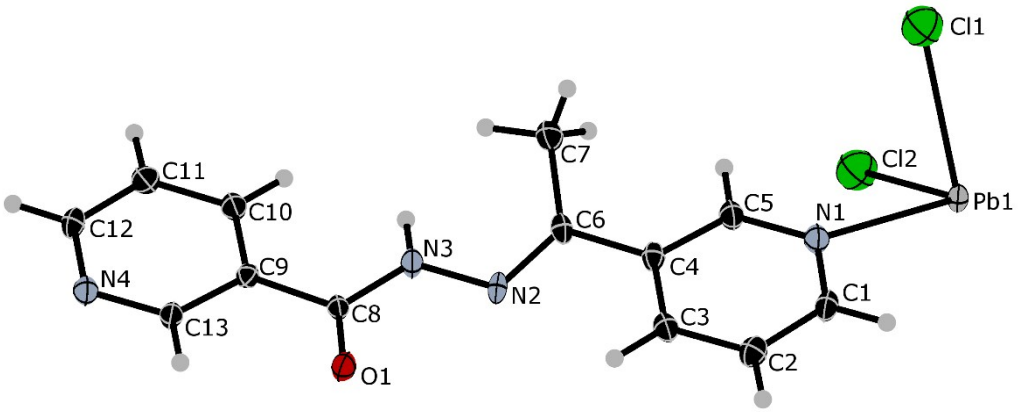

Fig. S9. Asymmetric unit of **822**. Thermal ellipsoids drawn with 50% probability.

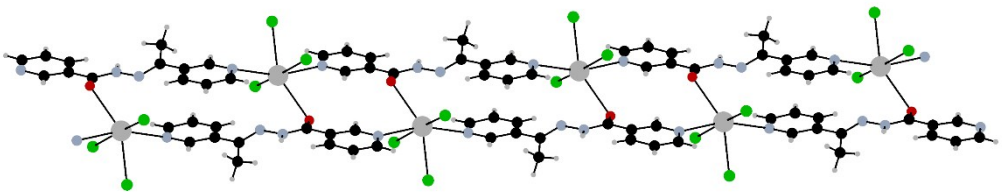

Fig. S10. Double coordination chain in the structure of **4**.

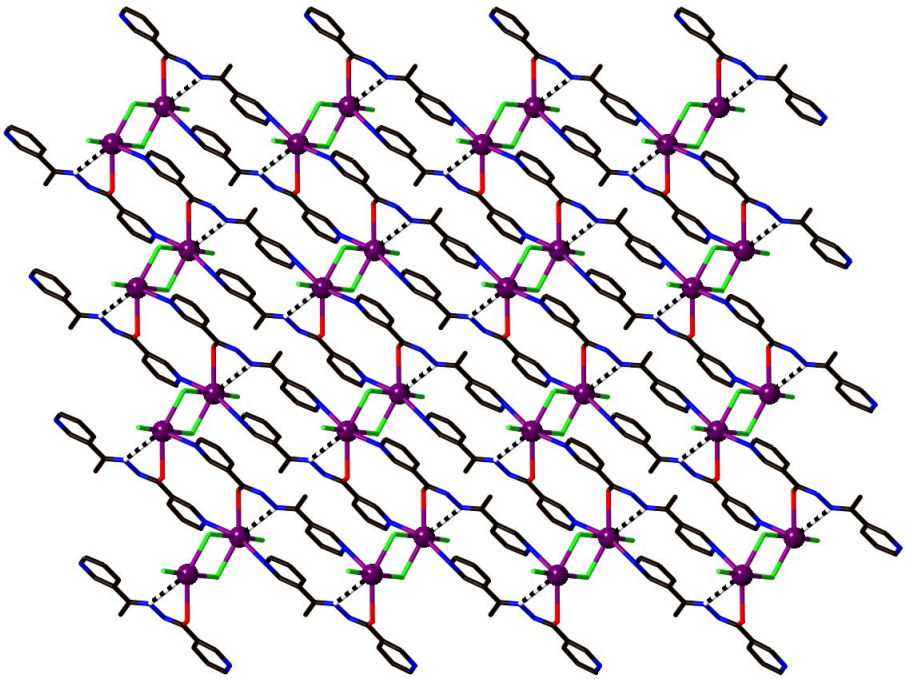

(a)

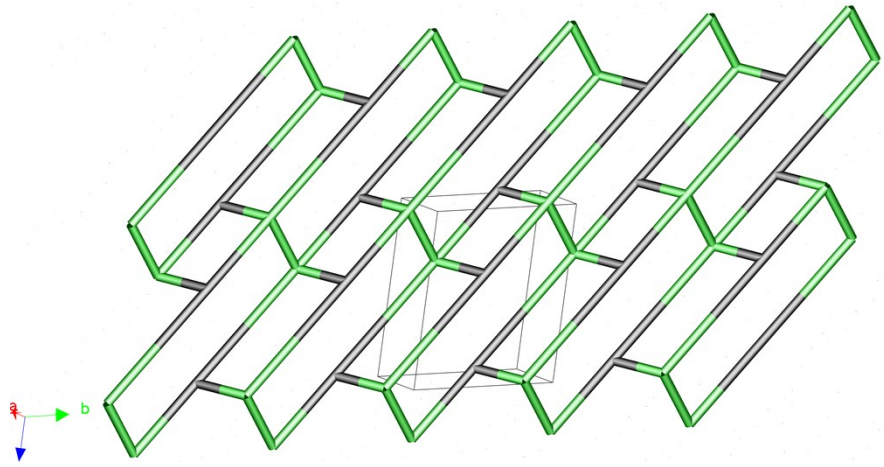

(b)

Fig. S11 (a). The 2D sheet structure of **4**; long Pb-N interactions higlighted by the striped bonds
(b) Schematic representation of 2D Sheet.

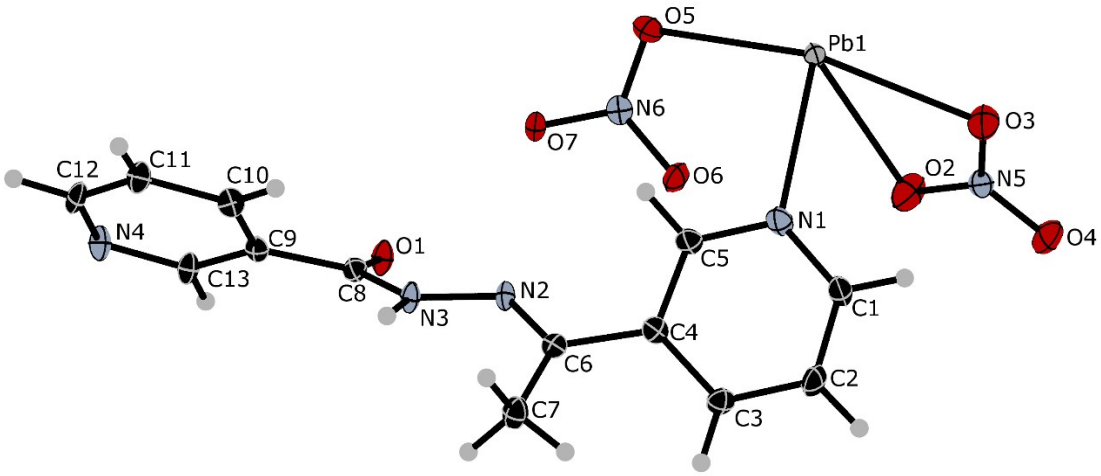

Fig. S12. Asymmetric unit of **5**. Thermal ellipsoids drawn with 50% probability.

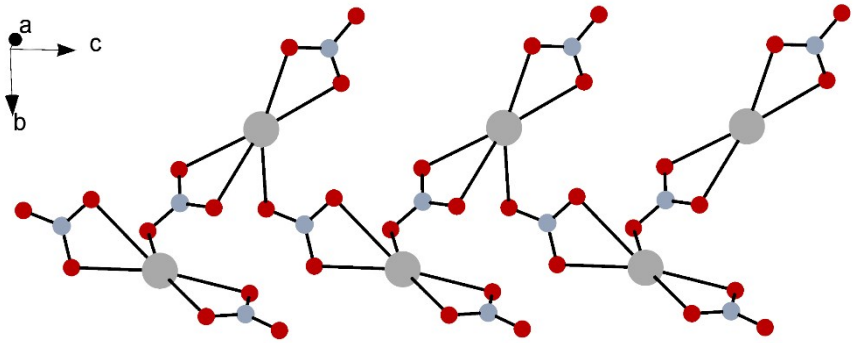

(a)

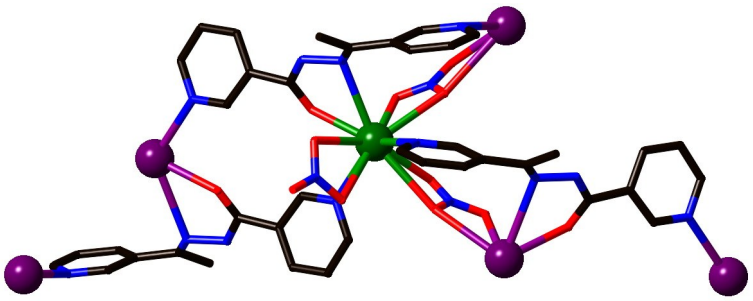

(b)

Fig. S13. (a) Fragment of a infinite 1D chain in **5 (b)** Local Pb, L2 and nitrate connectivity in **5** (Pb highlighted in green has complete coordination sphere shown).

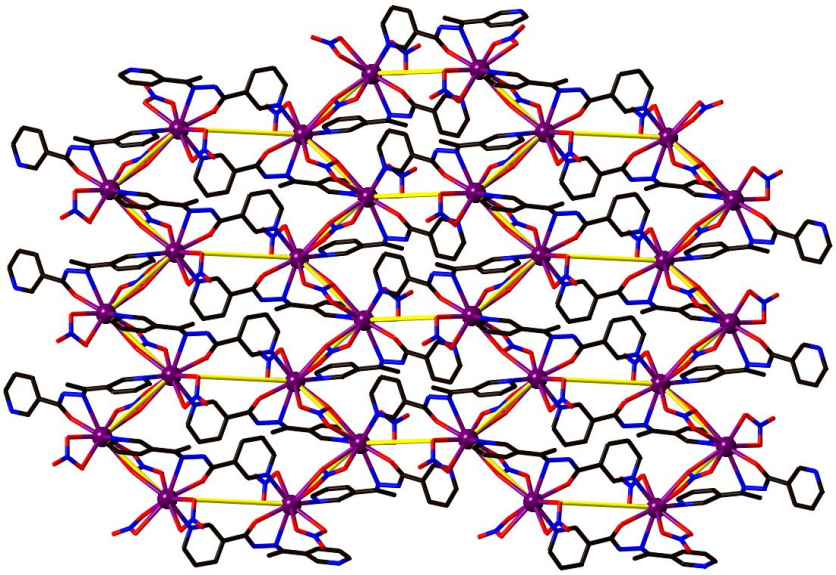

Fig. S14 The complicated 2D sheet formed in **5**; yellow bonds highlight the (6,3) connectivity.

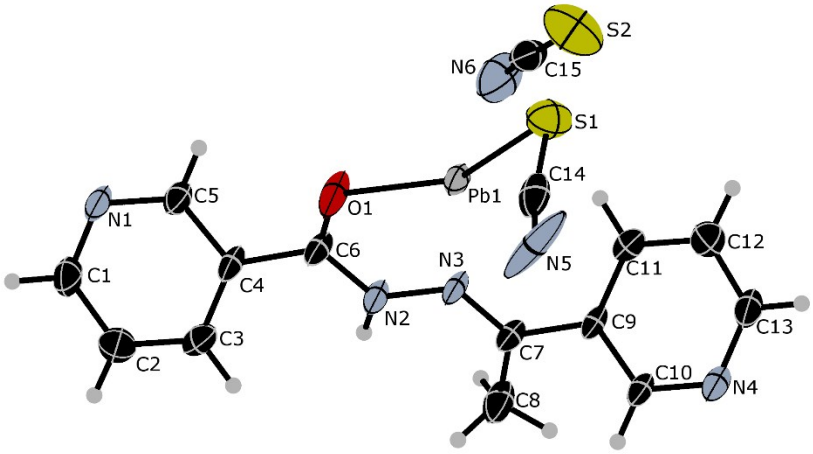

Fig. S15. Asymmetric unit of **6**. Thermal ellipsoids drawn in 50% probability

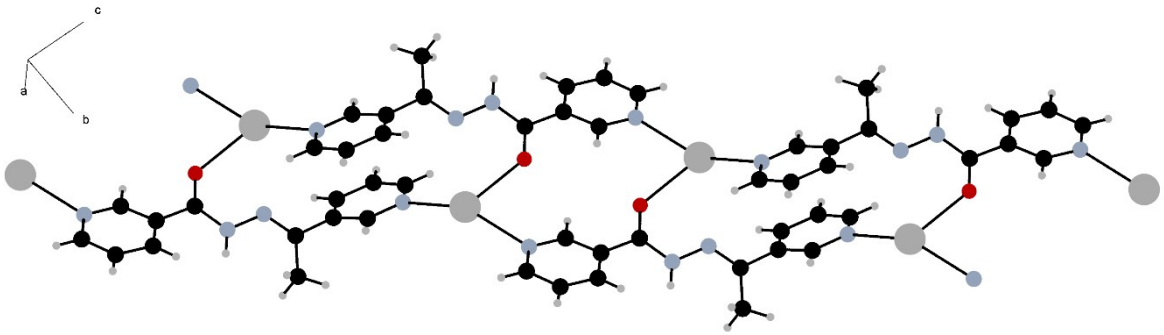

Fig. S16. Coordination chain in the structure of **6**.

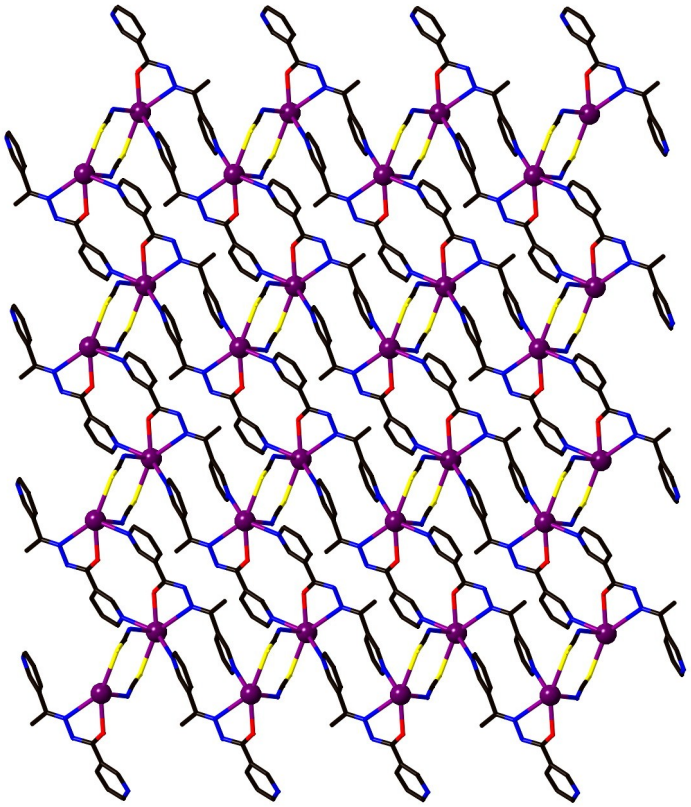

Fig. S17 The sheet structure of 6; further weakly bound monodentate SCN anions are omitted for clarity.

Detailed Hirshfeld surface analises.

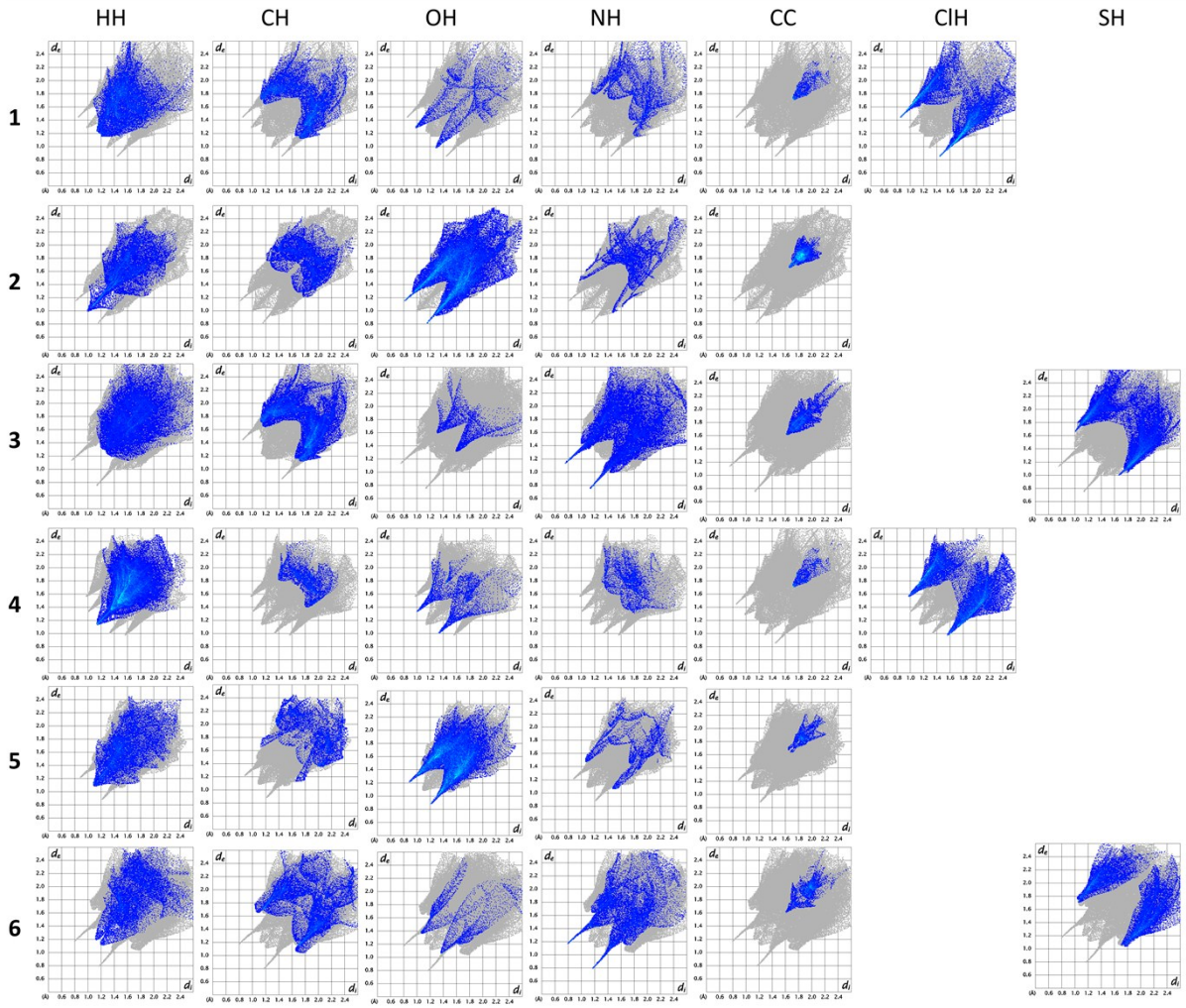

Fig. S18 Decomposition of Hirshfeld surfaces into contributions of main contacts for **1**-**6**.

On the Hirshfeld surface of a monomer of **1** fourteen red areas can be seen, apart from those arising crom the covalent Pb-Cl bonds connecting the monomeric units into a polymer, which are a consequence of one C–H···O bond (C13–H13···O1) and the remaining twelve are due to six C–H···Cl and N–H···Cl interactions (C4–H4···Cl2, C12–H12···Cl1, C11–H11···Cl2, C10–H10···Cl1, C7–H7C···Cl1 and N3–H3···Cl1). When shape index function is applied one can see large red 'hollows' indicating presence of C–H···π interactions. Analysis of decomposed fingerprint plots indicates that the most important types of interactions in packing in the structure of **1** are van der Waals forces (H···H, 24.0%), C–H···C and C–H···π interactions (21.0%) and weak hydrogen bonds involving chlorine ions (H···Cl, 24.6%).

Analysis of the Hirshfeld surface of the complex molecule of **2** mapped with d_{norm} function (combined with analysis of the 2D fingerprint plot indicates that the main type of interaction

taking part in the packing of molecules of **2** are hydrogen bonds in which oxygen atom acts as an acceptor (47.6% of the Hirshfeld surface). Several red areas on the Hirshfeld surface correspond to the presence of one strong hydrogen bond (N3-H3···O2) as well as five weaker ones (C10-H10···O1, C12-H12···O5, C13-H13···O4, C3-H3A···O5 and C4-H4···O6). The strong hydrogen bonds are evident in decomposed H···O fingerprint plot where are present two spikes. There are also red areas which are connected with the presence of H···H (C10-H10···H10^{i}-C10^{i}, where i: *–x*, *–y*, *–z*) and H···C (C13-H13···C13^{i}, where i: *–x*, *–y*, *–z*) contacts. The former constitute 17% of the Hirshfeld surface, the shortest one can be noticed on a decomposed H···H fingerprint plot as a central 'spike', while the latter make up 11.2% of the Hirshfeld surface. Two additional large red areas on the surface correspond to short Pb···N contacts (2.923 Å). When shape index function is used to map the surface, bow-tie motifs can be noticed which indicates presence of aromatic ring stacking interactions. This is consistent with bright spot on the decomposed C···C fingerprint plot.

When Hirshfeld surface of **3** is mapped with d_{norm} function sereval red areas can be noticed. They correspond to the existence of multiple strong N-H···N and weaker C-H···N, C-H···S hydrogen bonds as well as C-H···C interactions. H···N contacts (N6-H2N···N11, N2-H1N···N9, C14-H14C···N11, C25-H25···N10 mentioned above) constitute 18% of Hirshfeld. Short N-H···N hydrogen bonds are noticeable as long, sharp 'spikes' on the 2D plot. H···S hydrogen bonds make 19.1% of the surface, while other weak interactions, H···H and H···C constitute 20.4% and 19.7% of the Hirshfeld surface.

Because compound **6** is polymeric (like compound **1**) a segment of the structure has been chosen fo Hirshfeld surface analysis. Surface has been generated for part of the 1D chain containing two ligand molecules, two Pb^{2+} cations and two SCN^{-} ions. Since part of the chain is enveloped in the surface ten large red spots are visible on the surface mapped with d_{norm} function. Four of them are due to Pb-S tetrel bonds and six to Pb-N coordination bonds. From all other red areas two large ones stand out. They correspond to strong N-H···N hydrogen bond between ligand molecules and non coordinated SCN^{-} ions (N2-H2N···N6). There are also eight smaller red spots which presence is consistant with four weak C-H···X (X = N, S) hydrogen bonds (C8-H8A···N6, C3-H3···N6, C13-H13···S2, C8-H8A···S2). Several additional small red areas correspond to a number of C-H···C interactions (C11-H11···C15, C10-H10···H14, C8-H8···C15). When shape index function is applied 'bow-tie' patterns indicative of π···π stacking interactions as well as red hollow areas indicating C-H···π interactions are present (Fig. 11b). According to data from decomposed fingerprint plots van der Waals forces (18.2%), C-H···C interactions (19.9%) and weak C-H···X (X = S, N)

hydrogen bonds (H···N – 13.2% and H···S – 20.0%) constitute most of the forces responsible for packing of coordination chains in **6**. Asymmetry of decomposed fingerprint plots for H···C and H···N contacts is caused by the fact that the part of the chain inside the surface contains donor atoms for N-H···N hydrogen bonds and most donors of C-H···C interactions.

IR-spectra

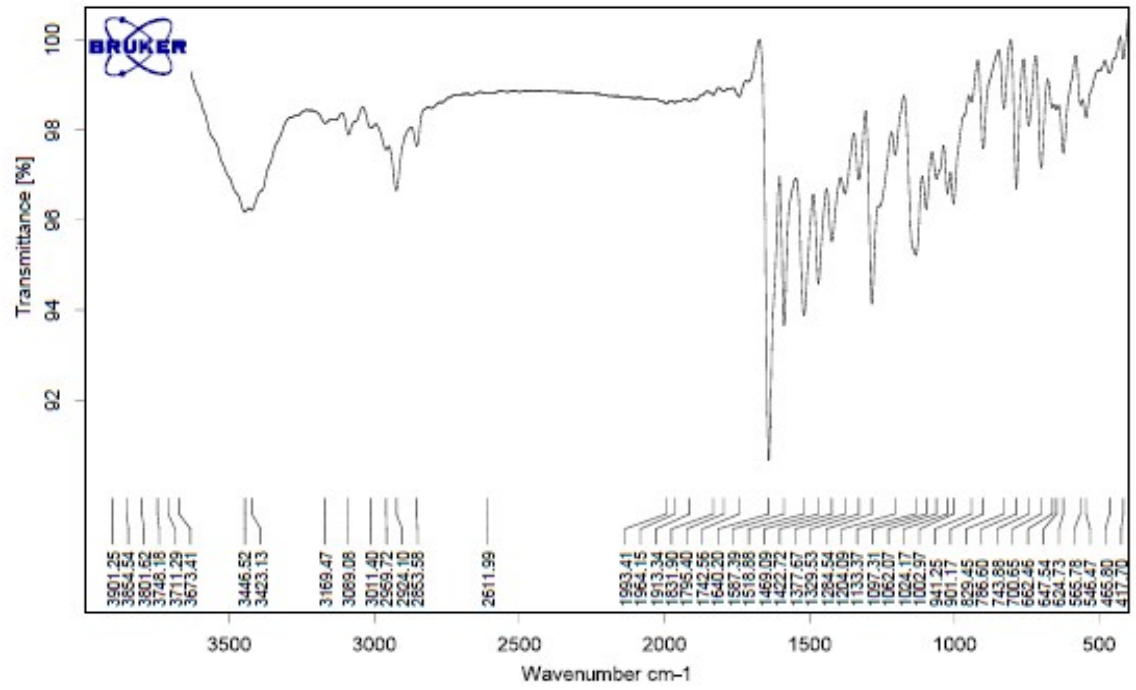

Fig. S19 IR spectrum of **1**.

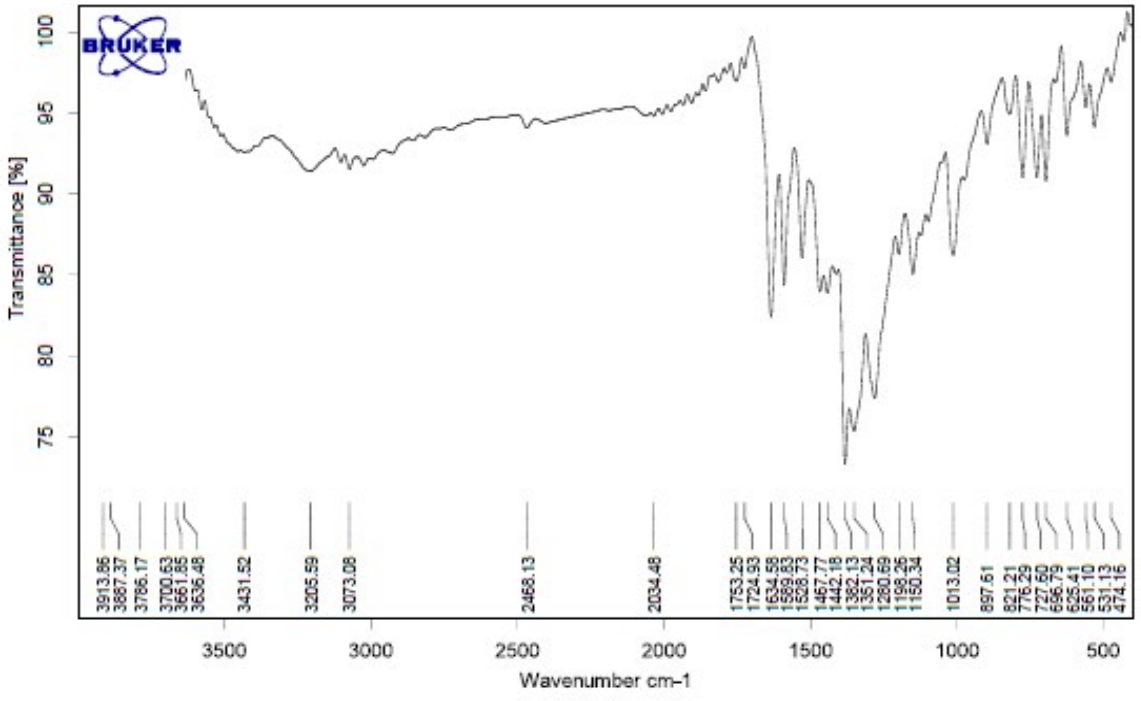

Fig. S20 IR spectrum of **2**.

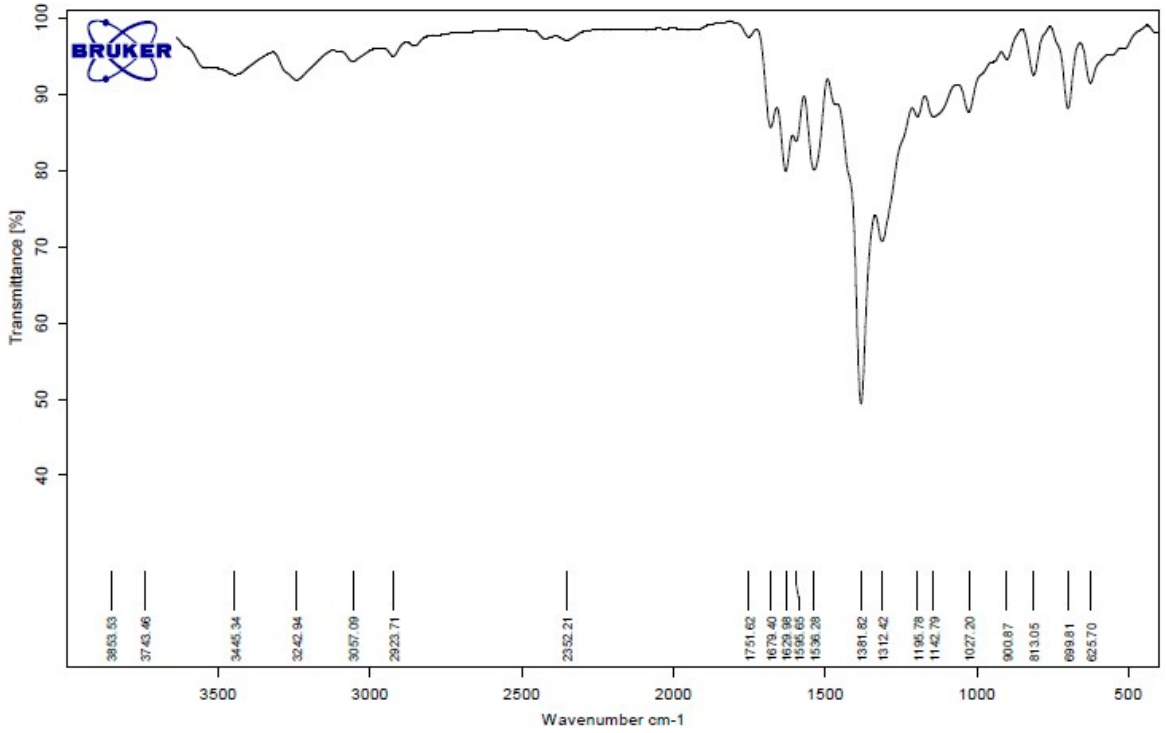

Fig. S21 IR spectrum of **5**.

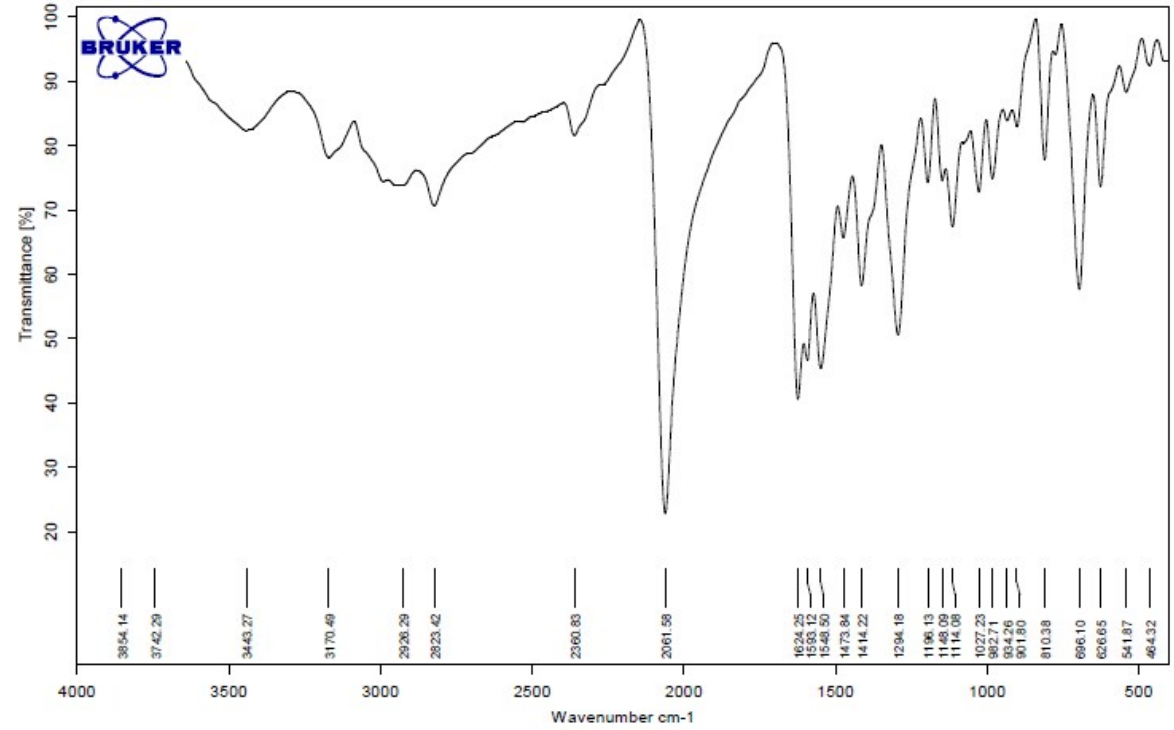

Fig. S22 IR spectrum of **6**.